IJEES

International Journal of Electrical Engineering and Sustainability (IJEES)

ISSN (online): 2959-9229

https://ijees.org/index.php/ijees/index

ISI 2023-2024: (0.557) Arab Impact Factor: 1.51 SJIF 2024 = 5.274

Volume 2 | Number 4 | October-December 2024 | Pages 12-18

Research Article

Enhancing Object Position Estimation Under GNSS Outages Through Kalman Filter Integration

Mohamad Abdalla [1*]

[1] Department of Telecommunication Engineering Technology, College of Electrical and Electronics Technology - Benghazi, Libya

*Corresponding author: mohamad.abdalla@ceet.edu.ly

Received: August 15, 2024 Accepted: November 06, 2024 Published: December 05, 2024

This is an open access article under the BY-CC license

Abstract: Determining the path and location of a person or vehicle using satellite navigation systems can be challenging or even impossible, particularly in areas where the satellite signal is weak or non-existent, such as inside tunnels and enclosed spaces. Consequently, tracking becomes difficult. To address this issue, a method has been researched to reduce the error rate in such locations: the Kalman Filter method. After implementing this approach, when the signal received from the satellites is strong, the application readings closely align with the satellite readings, making it applicable in areas where the satellite signal is either weak or nonexistent.

Keywords: Kalman filter, Global Navigation Satellite System, Object Tracking, Inertial Navigation System, State Estimation.

1. Introduction

In recent times and in the coming years, high precision in determining locations is crucial and sensitive, particularly in self-driving cars, drones, ships, and tracking children, as well as being significant in industry, health, and other sectors. From this, we recognize that tracking objects is vital in contemporary life and in the future to prevent accidents and enhance safety [1,2]. To achieve high accuracy in location determination, a combination of sensors with varying specifications is employed. Typically, artificial satellites and INS serve as the primary sources for location determination. While satellite systems offer high accuracy in open areas, the INS system can provide more comprehensive information, including location, direction, and speed [3,4]. To build an integrated navigation system by combining GNSS and INS data, the Kalman filter (KF) is typically employed. It has been demonstrated that the Kalman filter can provide accurate readings despite the noise from measurements [5,6]. bridges, in tunnels, or beneath dense trees and in valleys, the GNSS signal often becomes weak or non-existent. In such scenarios, the measurement noise is atypical and impacts the readings, making it challenging for autonomous satellite navigation systems to accurately determine location in complex environments [7,8].

The INS system functions as an auxiliary sensor for the GNSS system, particularly in enclosed spaces and tunnels, as it operates continuously without requiring external information. Over time, the accuracy of the GNSS system in determining location and tracking deteriorates due to the accumulation of errors, resulting in incorrect location information. Consequently, new methods must be implemented to address this issue. Location errors should be confined to a specific value and must ensure safety. Additionally, it is essential to consider interference from external sources and establish comprehensive safety systems to guarantee accurate and reliable readings that pose no risks [9,10].

This paper examines the application of the Kalman filter method and its comparison with GNSS readings in open areas with strong satellite signals. Participants walked in an open area on the Benghazi city track for 10 minutes, utilizing the MATLAB program to capture coordinate readings every second. Approximately 600 readings were recorded during this time, after which the GNSS path was plotted from the data. Subsequently, the Kalman filter method was employed to trace the path. It was determined that this path closely resembled the GNSS path, indicating its reliability in areas with weak or no coverage. The subsequent sections of this manuscript are organized as follows: Section 2 delineates the underlying mathematical framework of the Kalman filter, while Section 3 furnishes a comprehensive exposition of the corresponding algorithmic procedures. Section 4 presents and analyzes the simulation outcomes derived from the MATLAB implementation. Finally, concluding remarks are offered in the closing section.

2. Kalman filter

The Kalman filter is an efficient algorithm for estimating the state of a system from noisy measurements [11,12]. The goal of the Kalman filter is to take a probabilistic estimate of this state and update it in real time using two steps: Prediction and correction. Kalman filter requires the following motion and measurement models:

$$X_t = A_t X_{t-1} + B_t u_{t-1} + w_{t-1} \quad (1)$$

Where: X_t state of the system at time
A_t state transition matrix
B_t control matrix
w_t process noise
The estimate state at time step t is a linear combination of the estimate state at time t-1, control input at time t-1, and some zero noise. The input is an external signal that effect the evolution of the system state.

$$\mathrm{Z_t} = \mathrm{C_t X_t} + \mathrm{v_t} \quad (2)$$

Where:
Z_t is the measurement at time t
C_t is the measurement matrix
v_t is the measurement noise
The measurement noise $v_t \sim N(0, R_t)$, and the process noise $w_t \sim N(0, Q_t)$ are essential for determining the accuracy of our system and the uncertainty regarding the effects of control inputs. Once the researcher has established the aforementioned system, the subsequent methodology proceeds in two key phases. First, the motion model is employed to predict the state. Next, the measurement model is utilized to refine this forecast by incorporating measurement residuals (innovations) and applying the optimal gain. Ultimately, this iterative process continuously improves the estimated state through systematic integration of observed data.

3. Kalman Filter Algorithm

The equations of the Kalman filter are divided into two groups [13-15].

3.1 Prediction equation (prediction state)

$$X_t = A_t X_{t-1} + B_t u_{t-1} \quad (3)$$

Where:
X_t: predicted state estimate from time (t-1) to t
X_{t-1}: using state estimate from time (t-1)

$$P_{t/t-1} = A_t P_{t-1/t-1} A_t^T + Q_t \quad (4)$$

Where:
$P_{t/t-1}$: predicted error covariance from (t-1) to t
$P_{t-1/t-1}$: using error covariance at time (t-1)
Q_t: process variance matrix

3.2 Correction equations

$$K_t = P_{t/t-1}C_t^T(C_tP_{t/t-1}C_t^T + R_t)^{-1} \quad (5)$$

Where:

K_t: kalman gain

R_t: measurement variance

$$X_{t/t} = X_{t/t-1} + K_t\left(Z_t - C_tX_{t/t-1}\right) \quad (6)$$

Where:

$X_{t/t}$: update state estimate

Z_t: measurement

$C_tX_{t/t-1}$: predicated measurement

$Z_t - C_tX_{t/t-1}$: residual

$$P_{t/t}=P_{t/t-1} - K_tC_tP_{t/t-1} \quad (7)$$

Where:

$P_{t/t}$: updated error covariance

4 Simulation Results

Data acquisition was conducted by gathering sensor measurements and GNSS readings with the "MATLAB" mobile application during a 10-minute pedestrian traversal in an open area in Methmar, Tapalino, Benghazi. The inertial measurements from the IMU were subsequently employed to visualize the overall acceleration magnitude, as well as the individual accelerations along the three principal axes. These results are depicted in **Figures 1** (a–d).

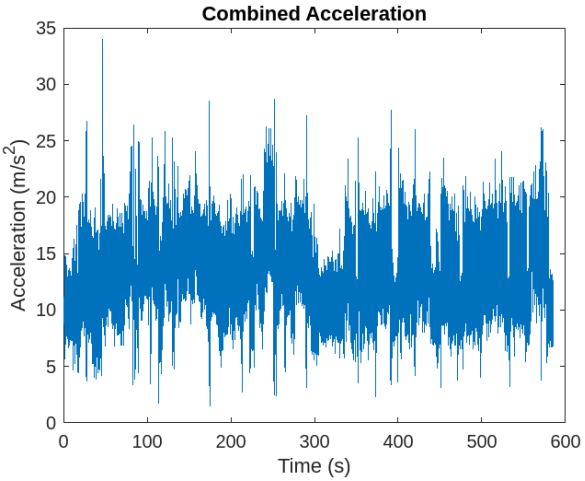

Figure 1. (a) combined acceleration.

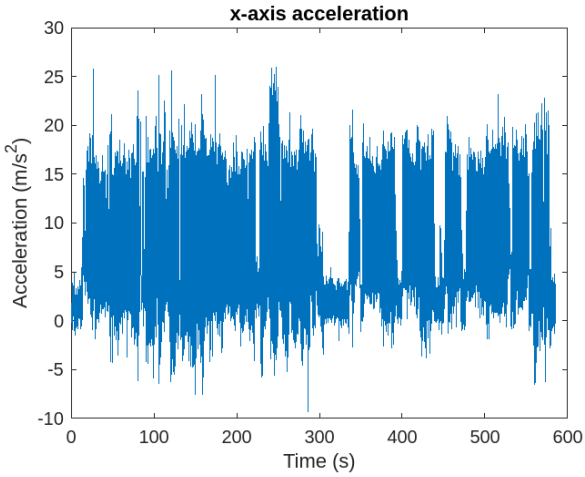

Figure 1 (b). x-axis acceleration

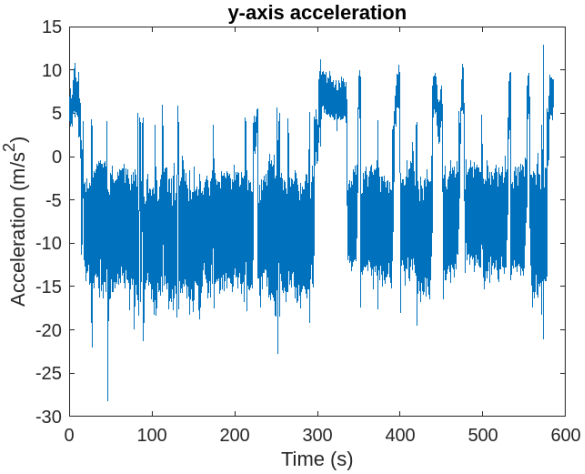

Figure 1 (c) y-axis acceleration

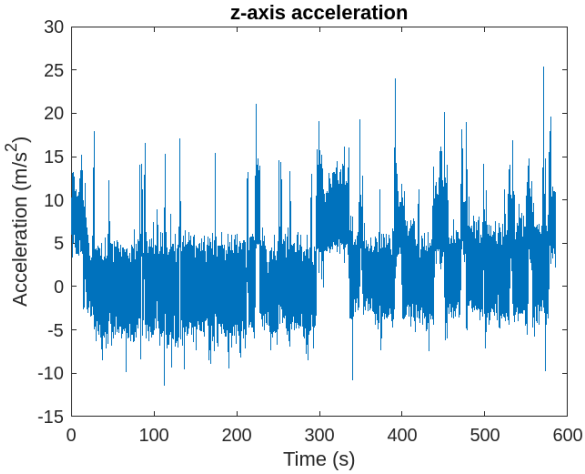

Figure 1 (d). z-axis acceleration.

Subsequently, the magnetic field, orientation, and angular velocity were each plotted along their respective three axes. These results are presented in Figures 2, 3, and 4, respectively.

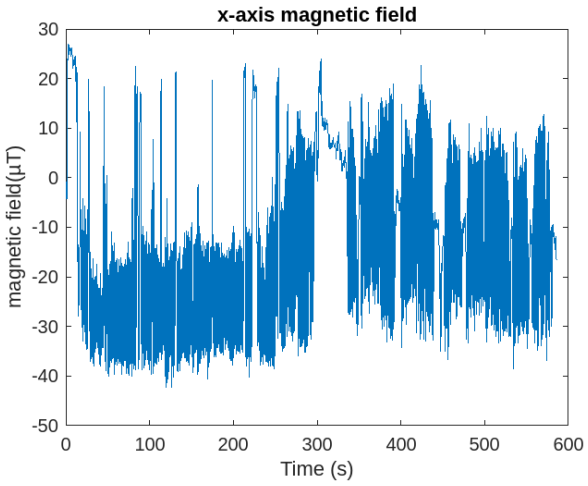

Figure 2 (a). x-axis magnetic field.

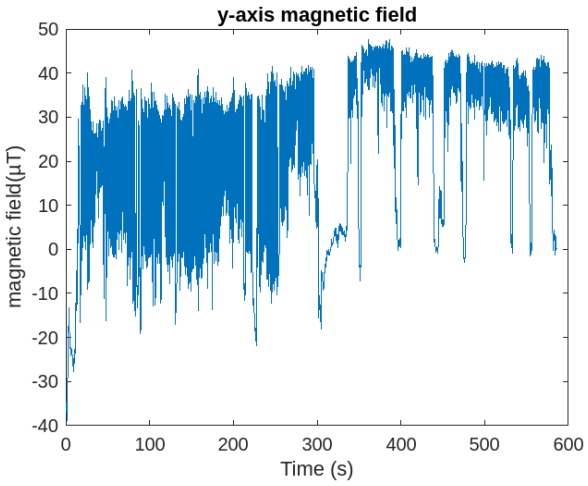

Figure 2 (b). y-axis magnetic field.

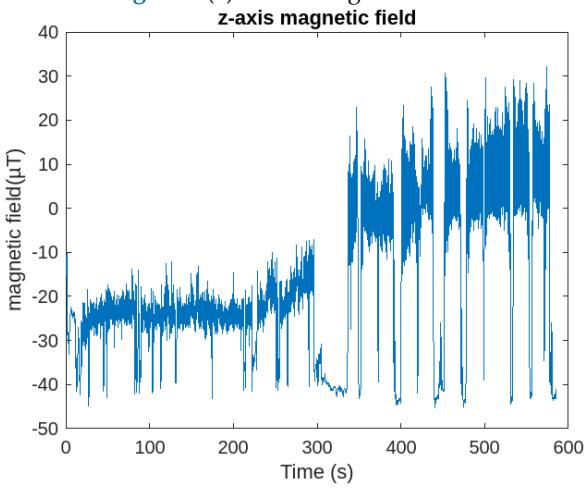

Figure 2 (c). z-axis magnetic field.

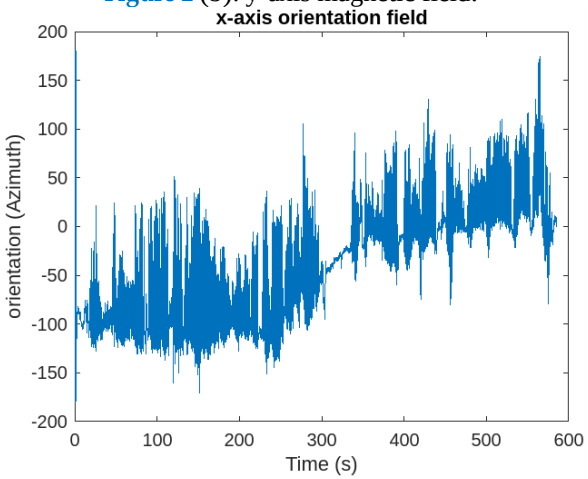

Figure 3 (a). x-axis orientation field.

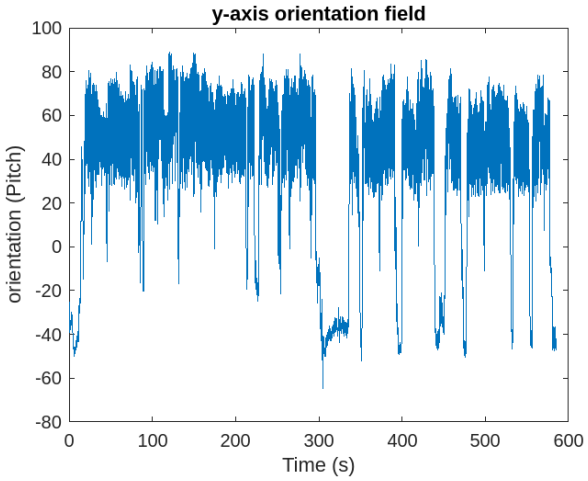

Figure 3 (b). y-axis orintation field.

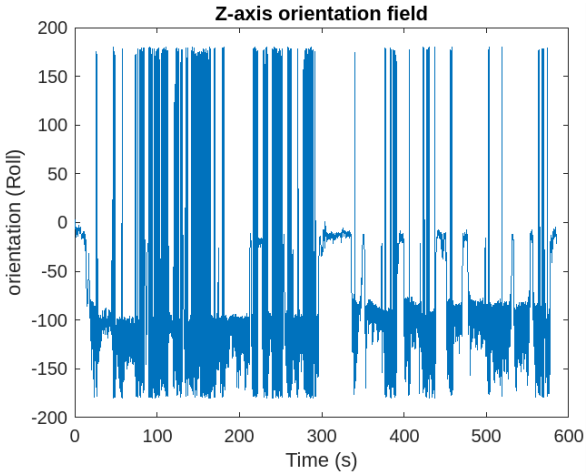

Figure 3 (c). z-axis orintation field.

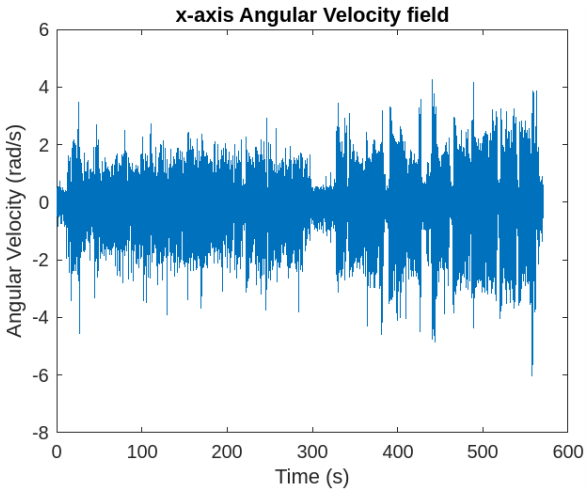

Figure 4 (a). x-axis angular velocity.

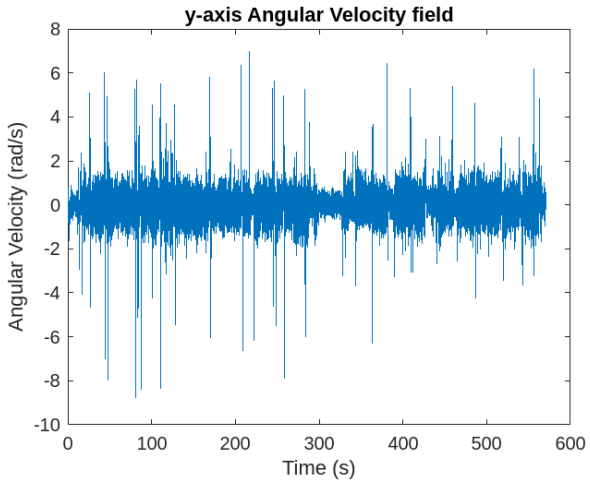

Figure 4 (b). y-axis angular velocity.

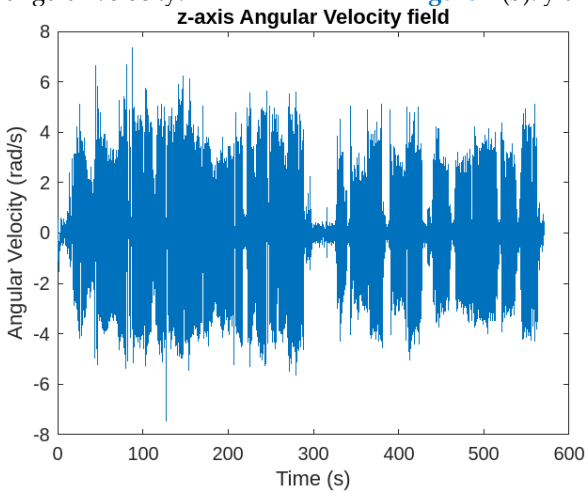

Figure 4 (c). z-axis angular velocity.

Collected location data compared to the Kalman filtered solution. Next, plot both the collected GNSS position (latitude, longitude) and the Kalman filter estimated position (latitude, longitude) on the web map, where the blue line represents the collected GNSS data and the red line indicates the estimated position from the Kalman filter, as illustrated in **Figures** 5 (a-b).

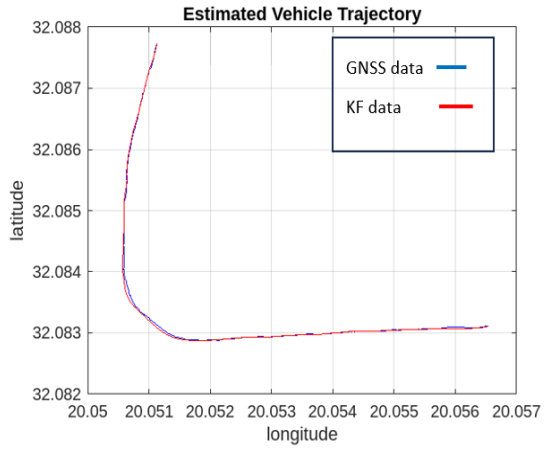

Figure 5 (a). Estimated vehicle Trajectory.

Figure 5 (b). Web map trajectory.

5. Conclusion

Accuracy in determining location and motorization is crucial for self-driving vehicles, particularly in areas lacking satellite coverage, such as tunnels, enclosed spaces, valleys, and cities with tall buildings. The Kalman filter was employed to address this issue, as it was tested in an area of Benghazi. Both satellite data and the Kalman filter were utilized to navigate, revealing that the two paths were remarkably similar. Consequently, Kalman filter technology can be trusted to ascertain the routes of self-driving cars, especially in urban environments where satellite signals are weak or absent.

Author Contributions: Author has contributed significantly to the development and completion of this article.

Funding: This article received no external funding.

Data Availability Statement: Not applicable.

Acknowledgments: The author would like to express their sincere gratitude to the Department of Telecommunication Engineering Technology, College of Electrical & Electronics Technology - Benghazi, Libya, for their invaluable support and resources throughout the course of this research. Their guidance and contributions have been instrumental in the successful completion of this work.

Conflicts of Interest: The author(s) declare no conflict of interest.

ORCID
Mohamad Abdalla https://orcid.org/0000-0001-9009-7608

References

[1] Y. Li, H. Yu, L. Xiao, and Y. Yuan, "Inspection robot GPS outages localization based on error Kalman filter and deep learning," *Rob. Auton. Syst.*, vol. 183, no. 104824, p. 104824, 2025. [Google Scholar]

[2] H. Jiao, X. Tao, L. Chen, X. Zhou, and Z. Ju, "GNSS/5G joint position based on weighted robust iterative Kalman filter," *Remote Sens. (Basel)*, vol. 16, no. 6, p. 1009, 2024. [Google Scholar]

[3] F. Liu, H. Zhao, and W. Chen, "A hybrid algorithm of LSTM and factor graph for improving combined GNSS/INS positioning accuracy during GNSS interruptions," *Sensors (Basel)*, vol. 24, no. 17, p. 5605, 2024. [Google Scholar]

[4] R. Jin, G. Zhang, L.-T. Hsu, and Y. Hu, "A survey on cooperative positioning using GNSS measurements," *IEEE Trans. Intell. Veh.*, pp. 1–20, 2024. [Google Scholar]

[5] S. I. K. Abdelaziz, H. Y. Elghamrawy, A. M. Noureldin, and G. Fotopoulos, "Body-centered dynamically-tuned error-state extended Kalman filter for visual inertial odometry in GNSS-denied environments," *IEEE Access*, vol. 12, pp. 15997–16008, 2024. [Google Scholar]

[6] R. Kumar Reddy Damagatla and M. Atia, "Improving EKF-Based IMU/GNSS Fusion Using Machine Learning for IMU Denoising," *IEEE Access*, vol. 12, pp. 114358–114369, 2024. [Google Scholar]

[7] S. Quan, S. Chen, Y. Zhou, S. Zhao, H. Hu, and Q. Zhu, "A robust position estimation method in the integrated navigation system via factor graph," *Remote Sens. (Basel)*, vol. 16, no. 3, p. 562, 2024. [Google Scholar]

[8] T. E. Tabassum, Z. Xu, I. Petrunin, and Z. A. Rana, "Integrating GRU with a Kalman Filter to enhance visual inertial odometry performance in complex environments," *Aerospace*, vol. 10, no. 11, p. 923, 2023. [Google Scholar]

[9] M. Khaleel *et al.*, "An optimization approaches and control strategies of hydrogen fuel cell systems in EDG-integration based on DVR technology," *J. Eur. Syst. Autom.*, vol. 57, no. 2, pp. 551–565, 2024. [Google Scholar]

[10] M. Tarek *et al.*, "Enhanced navigation precision through interaction multiple filtering: Integrating invariant and extended Kalman filters," *IEEE Access*, vol. 12, pp. 175357–175374, 2024. [Google Scholar]

[11] M. Khaleel, Z. Yusupov, Y. Nassar, H. J. El-khozondar, A. Ahmed, and A. Alsharif, "Technical challenges and optimization of superconducting magnetic energy storage in electrical power systems," *e-Prime - Advances in Electrical Engineering, Electronics and Energy*, vol. 5, no. 100223, p. 100223, 2023. [Google Scholar]

[12] Z. Wang, B. Li, Z. Dan, H. Wang, and K. Fang, "3D LiDAR aided GNSS/INS integration fault detection, localization and integrity assessment in urban canyons," *Remote Sens. (Basel)*, vol. 14, no. 18, p. 4641, 2022. [Google Scholar]

[13] S. Zhao, Y. Zhou, and T. Huang, "A novel method for AI-assisted INS/GNSS navigation system based on CNN-GRU and CKF during GNSS outage," *Remote Sens. (Basel)*, vol. 14, no. 18, p. 4494, 2022. [Google Scholar]

[14] R. Zhai and Y. Yuan, "A method of vision aided GNSS positioning using semantic information in complex urban environment," *Remote Sens. (Basel)*, vol. 14, no. 4, p. 869, 2022. [Google Scholar]

[15] N. Boguspayev, D. Akhmedov, A. Raskaliyev, A. Kim, and A. Sukhenko, "A comprehensive review of GNSS/INS integration techniques for land and air vehicle applications," *Appl. Sci. (Basel)*, vol. 13, no. 8, p. 4819, 2023. [Google Scholar]


Open Access This article is licensed under a Creative Commons Attribution 4.0 International License, which permits use, sharing, adaptation, distribution and reproduction in any medium or format, as long as you give appropriate credit to the original author(s) and the source, provide a link to the Creative Commons licence, and indicate if changes were made. The images or other third-party material in this article are included in the article's Creative Commons licence, unless indicated otherwise in a credit line to the material. If material is not included in the article's Creative Commons licence and your intended use is not permitted by statutory regulation or exceeds the permitted use, you will need to obtain permission directly from the copyright holder. To view a copy of this licence, visit http://creativecommons.org/licenses/by/4.0/.

© The Author(s) 2024